

RSC Advances



This is an *Accepted Manuscript*, which has been through the Royal Society of Chemistry peer review process and has been accepted for publication.

Accepted Manuscripts are published online shortly after acceptance, before technical editing, formatting and proof reading. Using this free service, authors can make their results available to the community, in citable form, before we publish the edited article. This *Accepted Manuscript* will be replaced by the edited, formatted and paginated article as soon as this is available.

You can find more information about *Accepted Manuscripts* in the [Information for Authors](#).

Please note that technical editing may introduce minor changes to the text and/or graphics, which may alter content. The journal's standard [Terms & Conditions](#) and the [Ethical guidelines](#) still apply. In no event shall the Royal Society of Chemistry be held responsible for any errors or omissions in this *Accepted Manuscript* or any consequences arising from the use of any information it contains.

ARTICLE

A Novel pH-Responsive POSS-Based Nanoporous Luminescent Material Derived from Brominated Distyrylpyridine and Octavinylsilsesquioxane

Cite this: DOI: 10.1039/x0xx00000x

Wenyan Yang,^a Xuesong Jiang,^{*b} Hongzhi Liu^{*a,c}Received 00th January 2012,
Accepted 00th January 2012

DOI: 10.1039/x0xx00000x

www.rsc.org/

For the first time, a novel pH-responsive porous material based on POSS was easily prepared from the cubic octavinylsilsesquioxane (OVS) and brominated distyrylpyridine (Br-DSP) *via* the Heck coupling reaction. The resulting material possessed high porosity with Brunauer–Emmett–Tellerspecific surface area of 600 m² g⁻¹ and total pore volume of 0.58 cm³ g⁻¹. It also exhibited high CO₂ storage capability of 0.82 mmol g⁻¹ (3.62 wt %) at 298 K/760 Torr. The porous polymer was luminescent with the maximum emission at ca. 530 nm in the solid state, due to the incorporation of the conjugated structures of distyrylpyridine. Owing to the protonated nitrogen centers in the porous material, excellent pH-responsive property was observed and a linear relation was established between the maximum luminescent emission wavelengths (λ_{em}) of the turbid liquid in buffer solutions and the corresponding pH values in the pH range from 1 to 4. This porous material is very promising as a fluorescent probe in the rapid test systems.

Introduction

Porous materials with novel intrinsic properties such as high specific surface area, excellent porosity and good thermal stability have potential applications in gas storage and separation,¹ optical devices,^{2,3,4} heterogeneous catalysis,⁵ *etc.* Covalently-linked porous polymers have attracted specific interest because their structures and properties are easily tuned through rational design.⁶ By selecting the ideal building blocks and proper chemical reactions, an excellent porous polymer can be efficiently produced. Usually, functional building blocks with rigid structures are selected to form stable pores in the crosslinked polymer, which prevent the skeleton from collapsing.⁷ In addition, the functional building blocks could endow the porous material with many novel properties.^{7,8,9}

Recently, functional fluorescent porous polymers with intrinsic fluorescence and three-dimensional (3D) network structures^{10,11} have been extensively investigated. Some of these polymers were successfully prepared by selecting monomers with rigid, contorted structures and π -electronic conjugated components,¹⁰⁻¹⁴ such as spirobifluorene,^{2,15} phenyl,¹⁶ carbazole,¹⁷ pyrene,¹⁸ and tetraphenylethene^{19,20} units.

Polyhedral oligomeric silsesquioxanes (POSS), with a rigid 3D nanometer-sized inorganic-organic hybrid structures are particularly suitable building blocks to construct porous polymers.^{21,22} Many porous polymers derived from POSS have been prepared *via* polymerizations reactions including hydrosilylation,²³ Sonogashira coupling reaction,²⁴ Yamamoto coupling reaction,²⁵ Heck reaction^{26,27} and Friedel–Crafts reaction,²⁸⁻³⁰ radical polymerization^{31,32} and others.^{33,34} By utilizing their rigid and bulky cages, POSS can increase the

quantum yields of fluorescent molecules or polymers due to their enhanced aggregation prevention of dye molecules and the inhibition of self-quenching in the solid state.³⁵⁻³⁷ However, POSS-based luminescent porous materials have rarely been investigated so far, and the development of novel fluorescent porous polymers based on POSS could be a promising field in the future.

The design and application of various sensing porous materials, which respond to outer stimulus such as changes in pH, luminosity and temperature, have become one of the focuses in the field of environmentally, biologically and medically oriented chemical analysis.³⁸ Some pH responsive porous materials such as porous glass,³⁹ hydrogel-capped porous SiO₂⁴⁰ and nanoporous silica colloidal membranes have been reported.⁴¹ However, up to date, all of the pH responsive porous materials were obtained by physically absorbing the pH responsive molecules.⁴²⁻⁴⁶ The resulting interactions were relatively weak and the responsive molecules easily fell off from the porous materials. Therefore, it was imperative to develop a novel pH responsive porous polymer where the responsive molecules are covalently-linked within the materials matrix.

Distyrylpyridine (DSP) analogs are pyridine derivatives with structurally fixed styryl moieties and they are a novel class of fluorescence materials.⁴⁷ Their structural rigidity would endow them with high fluorescence quantum yields and nitrogen atoms in the pyridine moieties would be potential protonated centers. These characteristics make them potential sensing materials because the protonation of the rather effective fluorophores leads to pronounced changes in fluorescence spectra.⁴⁸⁻⁵⁰ Some excellent pH-sensing materials based on DSP derivatives have

been prepared through the non-covalent immobilization of these dyes on silica. Due to the insolubility of DSPs in water, they could be applied in the analysis of aqueous media. However, these dyes probably fell off from silica while performing the analysis of organic media.

Considering the structural rigidity of DSP, some novel functional DSP derivatives could be designed and synthesized and they could act as rigid building blocks to construct covalently-linked porous materials to overcome the above-mentioned limitations through non-covalent adsorption.⁵¹⁻⁵³ In this paper, for the first time, we have synthesized brominated distyrylpyridine (Br-DSP) through one-step reaction, which was confirmed by NMR, FTIR and mass spectrum (Supporting information).

It was expected that this novel fluorescent molecule (Br-DSP) could react with octavinylsilsesquioxane (OVS) to construct hybrid nanoporous polymer *via* the Heck reaction. Thus, the distyrylpyridine rigid structure was covalently incorporated into POSS-based porous material. This hybrid porous polymer (HPP) is hopeful to keep the excellent pH-sensing property and has promising and wide applications in the rapid detecting system.

Experimental section

Materials: Unless otherwise noted, all reagents were purchased from commercial suppliers and used without further purification. Octavinylsilsesquioxane (OVS) was synthesized as the previous reports.^{54,55} Br-DSP was synthesized through one-step reaction according to our previous report.⁴⁷ *N,N*-dimethylformamide (DMF) was dried over CaH₂ at 80 °C for 12 h and distilled under vacuum pressure, then stored with 4 Å molecule sieves prior to use. Triethylamine (Et₃N) was dried by distillation over CaH₂ and used freshly.

Measurements: Fourier-transform infrared (FT-IR) spectra of the products were recorded on a Bruker Tensor 27 spectrophotometer from 4000 to 400 cm⁻¹. Solid-state ²⁹Si MAS NMR and ¹³C CP/MAS NMR spectra were performed on a Bruker AVANCE-500 NMR Spectrometer operating at the resonance frequencies of 125 MHz for ¹³C and 99 MHz for ²⁹Si under a magnetic field strength of 9.4 T. A chemagnetics of 5 mm triple-resonance MAS probe was used to acquire ¹³C and ²⁹Si NMR spectra. ²⁹Si MAS NMR spectra with high power proton decoupling were recorded using a $\pi/2$ pulse length of 5 μ s, a recycle delay of 120 s and a spinning rate of 5 kHz. Elemental analyses were conducted by using an Elementarvario EL III elemental analyzer. The pH of the buffer solutions was controlled by the universal pH meter PHS-3C with the glass electrode ESL-11g-05, which was calibrated by the standard aqueous buffer solutions (Leici, Shanghai). Luminescence (excitation and emission) spectra were determined with a Hitachi F-4500 spectrophotometer.

Field-emission scanning electron microscopy (FE-SEM) tests were performed by using a HITACHI S4800 spectrometer. The high-resolution transmission electron microscopy (HR-TEM) experiments were recorded on a JEM 2100 electron microscope (JEOL, Japan) with an acceleration voltage of 200 kV. Thermal gravimetric analyses (TGA) were measured on a Mettler-Toledo TGA/DSC system under nitrogen at 10 °C/min to 800 °C. Powder X-ray diffraction (PXRD) were performed on a Rigaku D/MAX 2550 diffractometer with Cu-K α radiation, 40 kV, 200 mA with the 2 θ range of 10°-80° at room temperature.

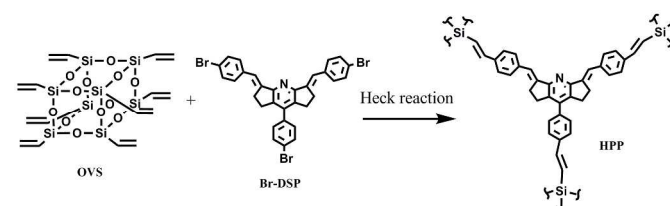
Nitrogen sorption isotherm measurements were recorded by using a Micro Meritics surface area and pore size analyzer. The

samples were degassed at 160 °C for 12 h prior to measurement. A sample of ca. 0.1g and a UHP-grade nitrogen (99.999%) gas source were selected in the nitrogen sorption measurements at 77 K and collected on a Quantachrome Quadrasorb apparatus. BET surface areas were evaluated at a *P/P*₀ range of 0.01 to 0.20. Nonlocal density functional theory (NL-DFT) pore size distributions were performed on the carbon/slit-cylindrical pore mode of the Quadrawin software.

Synthesis of hybrid porous polymers (HPP): An oven-dried flask was added OVS (211 mg, 0.33 mmol), Br-DSP (576 mg, 0.89 mmol), palladium acetate (34 mg, 0.15 mmol) and tris(2-methylphenyl)phosphine (91 mg, 0.30 mmol) in DMF/Et₃N (45 mL/15 mL) under argon. The mixture was bubbled by argon under stirring for 30 min at room temperature and then heated at 100 °C for 48 h. After cooling to room temperature, the mixture was filtered and washed with water, THF, methanol, chloroform and acetone to remove the remnant amine salts, residuary monomers and catalyst. The products were further purification under the Soxhlet extractor with THF for 24 h and methanol for 24 h, and dried in vacuo at 70 °C for 48 h. HPP was afforded as a kelly solid (578 mg). Yield: 101%. Elemental analysis calc. (wt.%) for Si₁₂₄O₃₆C₂₉₆H₂₂₄N₈: C 69.13, H 4.39, N 2.18. Found C 63.52, H 5.07, N 2.14.

Results and discussion

As shown in Scheme 1, HPP was prepared through the Heck reaction of OVS and Br-DSP in *N,N*-dimethylformamide (DMF) at 100 °C for 48 h. A highly crosslinking network was formed after the cross-coupling reaction, which favoured formation of pores and the resulting hybrid materials did not dissolve in most common solvents, for example, THF, chloroform, methanol and ethanol etc. Unlike non-covalent immobilization of DSP dyes on silica, these dye units keep stable in the network while performing the analysis of organic media.



Scheme 1. The synthetic route of HPP.

The structure of HPP was confirmed by FTIR, solid-state ¹³C cross polarization/magic angle spinning (CP/MAS) NMR and ²⁹Si MAS NMR spectroscopy. FTIR spectrum of HPP showed that the C=C stretching vibration peaks of ethylene and aryl groups for HPP were observed at 1412, 1510 and 1601 cm⁻¹; the strong peak at 1124 cm⁻¹ was assigned to the -Si-O-Si- stretching vibrations, which confirmed the existing POSS cages in HPP (Figure 2S).⁵⁶ There existed C=C, -Si-O-Si- and aryl groups simultaneously, indicating the presence of cross-linking networks in the hybrid polymer.

The solid-state ²⁹Si NMR spectrum of HPP showed signals at -62.4, -68.2 and -79.9 ppm, respectively (Figure 1), which were attributed to the silicon atoms of T₁, T₂ and T₃ units (T_n: CSi(OSi)_n(OH)_{3-n}) in the resulting network. T₃ unit arose from the unreacted Si-CH=CH₂ units and the resulting Si-CH=CH-Ar- units after the Heck reaction. The presence of T₁ and T₂ units indicated that partial POSS cages cleaved during the synthesis. This could be caused by three reasons. First, excessive Et₃N was added as the acid absorbent in the Heck

reaction, which could rupture the siloxane bonds. Second, HBr was formed during the synthesis. Although acid absorbent was added, the resulting HBr still may be a potential factor to cleave POSS cages. The third factor is that the rigid or straight structures could cause partial collapse of the POSS cages during the release of structural stress in the network. This result confirmed the existence of intact POSS moieties and partial POSS cages distorted, which was accorded with other porous polymers derived from POSS.^{25,57,58} Nevertheless, nearly 70% of POSS cages were remained intact according to the relative intensity ratios of T_3 signal, $T_3/(T_1+T_2+T_3) = 0.697$.

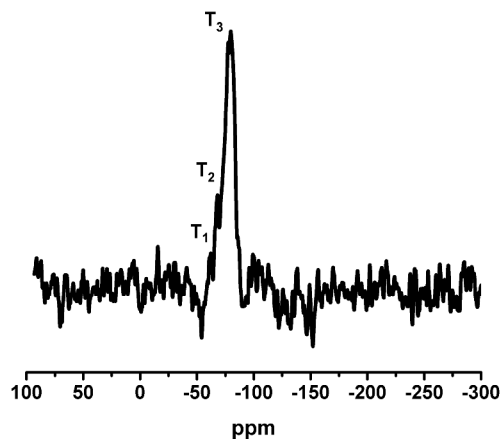


Figure 1. Solid-state ^{29}Si MAS NMR spectrum of HPP.

The Solid-state ^{13}C CP/MAS NMR spectra of HPP and Br-DSP were also analyzed in this work (Figure 2). Compared with Br-DSP, the ethylene units of HPP were formed through Heck reactions showed peaks at $\delta = 128$ and 159 ppm. The signals of aryl and unreacted vinyl carbon atoms were observed at $\delta = 93 \sim 142$ ppm, and the signals of saturated carbon atoms approached pyridine ring exhibited multiple peaks and displayed at $\delta = 0 \sim 37$ ppm, corresponding with the peaks of Br-DSP. The carbon atoms of the pyridine ring were observed at 190 and 196 ppm, which showed shifted to low field because the ethylene units extending the length of the conjugated system.

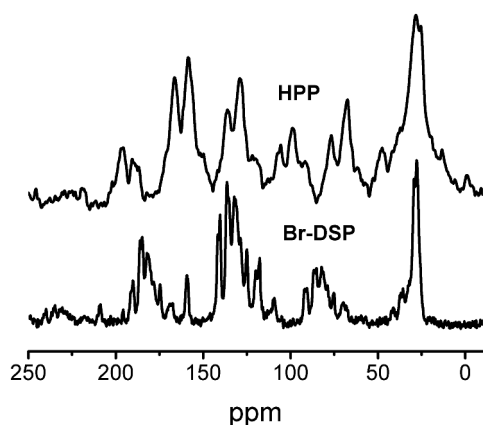


Figure 2. Solid-state ^{13}C CP/MAS NMR spectra of HPP and Br-DSP.

The porous properties of HPP were evaluated by nitrogen adsorption and desorption measurements at 77 K. HPP exhibited a sharp uptake at low relative pressures and gradually increasing uptake at higher relative pressures with a

inconspicuous hysteresis in Figure 3, suggesting the presence of micropores and mesopores simultaneously.^{26,27,29,30} The surface area of HPP was ascertained by the specific Brunauer–Emmett–Teller surface areas (S_{BET}) method. S_{BET} of HPP was calculated as $603 \text{ m}^2 \text{ g}^{-1}$ and the micropore surface area was calculated as $347 \text{ m}^2 \text{ g}^{-1}$ by t -plot method. Pore size distribution of the polymer was confirmed from the nonlocal density functional theory (NL-DFT). The result was accorded with the consequence of the N_2 isotherm and indicated the presence of micropores and mesopores within structures. As shown in Figure 3, HPP manifested the uniform micropores with an average diameter centered at about 1.54 nm and a broad distribution range of mesopores. The total pore volume (V_{total}) of HPP was $0.58 \text{ cm}^3 \text{ g}^{-1}$ and the ratio of the micropore volume (V_{micro}) to the V_{total} was 0.27 .

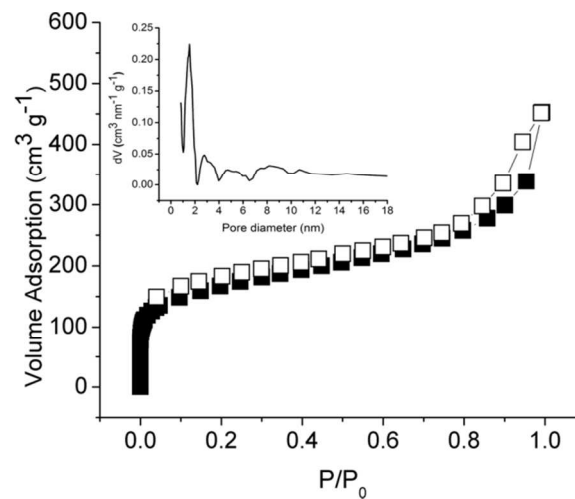


Figure 3. Nitrogen sorption isotherm and NL-DFT pore size distribution of HPP.

The thermal stability of the polymer was evaluated by thermogravimetric analysis (TGA) under N_2 at $10 \text{ }^\circ\text{C min}^{-1}$ from $45 \text{ }^\circ\text{C}$ to $800 \text{ }^\circ\text{C}$. HPP possessed good thermal stability and the mass remained invariant up to approximately $440 \text{ }^\circ\text{C}$ (decomposition temperature at 5 wt \% mass loss), which was significantly more stable than OVS and Br-DSP due to highly cross-linking networks (Figure 3S). The initial mass loss of HPP can be attributed to the breakage of organic moieties such as residual vinyl and phenyl groups. The decomposition that occurred at about $510 \text{ }^\circ\text{C}$ may be derived from the rupture of the siloxane spacers.^{26-30,57}

Although OVS is highly crystalline, powder X-ray diffraction (PXRD) patterns showed that the HPP was amorphous with no long-range crystallographic order and showed broad diffraction peaks at $\sim 22^\circ 2\theta$, which may be assigned to Si–O–Si linkages (Figure 4S).^{26-30,34}

The particle size and morphology were observed by field emission scanning electron microscopy (FE-SEM). HPP was shown the structure consisted of inter-linking irregular shapes with a wide size distribution range from 100 nm to tens of micrometers, in accordance with the consequence of PXRD (Figure 5Sa).^{26,27,29} The texture and ordering of HPP was evaluated by high-resolution transmission microscopy (HR-TEM). HR-TEM image confirmed the porous characteristics of HPP with a relatively uniform pore diameter. HPP was stable under the electron beam (Figure 5Sb).

Carbon dioxide storage is one of the potentially important applications for porous materials. And some of those porous materials based on POSS have been tested for CO_2

storage.^{30,31,58} It is interesting to investigate the CO₂ storage capacity for HPP after the introduction of pyridine groups into the hybrid network based on POSS. As shown in Figure 4, the CO₂ storage capacity for HPP was 0.82 mmol g⁻¹ (3.62 wt %) at 298 K/760 Torr. This result was comparable or higher than the corresponding values of other porous polymers based on POSS with higher S_{BET} than HPP.^[29,30] This relatively high CO₂ uptake capacity might be ascribed to the high affinity towards CO₂ through the strong dipole–dipole interaction and acid–base interaction by protonated and deprotonated states of the pyridine rings.^{59–62}

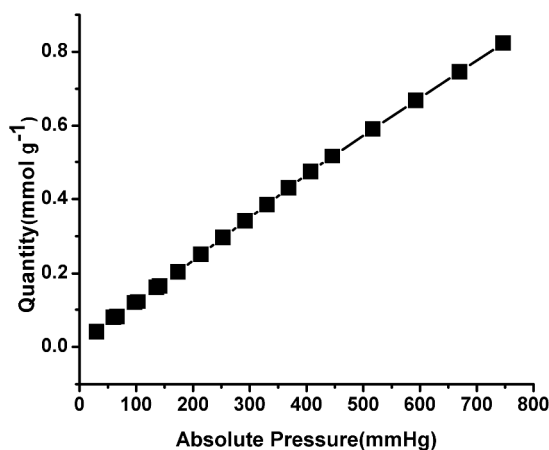


Figure 4. CO₂ adsorption isotherm at 298 K.

From the above-mentioned results, we know that the simultaneous introduction of the structural rigidity of bulky POSS cage and DSP structure make HPP possess good porosity and thermal stability. Moreover, the possible protonation of the highly basic nitrogen atom of pyridine moiety would result in substantial changes in fluorescence spectra and this feature could be used in the design of new fluorescence pH sensors.

Firstly, it is necessary to know whether the luminescence of HPP changes or not after the introduction of the structure of DSP units into the porous network. Compared with the luminescent spectrum of Br–DSP, HPP exhibited the similar maximum emission wavelength (λ_{em}) at ca. 530 nm (Figure 6S). It was a typical characteristic of green emitting materials. The emission can be assigned to the π – π^* transition including the aryl, ethylene groups, pyridyl groups in DSP and the POSS cages elicit limited effects on the π systems.^{27,35,36,63} This indicated that the fluorescent property of HPP derived from the structure of DSP was almost unaffected and some typical properties of DSP could be also utilized for HPP, for example, the remarkable pH response.

In order to investigate the pH–response of HPP, a series of buffer solutions were prepared on the base of the distilled water, acids, bases and salts solutions, *i.e.* oxalic acid and potassium oxalate (for pH range 1.00 – 2.50), citric acid and disodium hydrogen phosphate (for pH range 3.00 – 8.00) and glycolic acid and sodium hydroxide (for pH range 8.50 – 12.00) with the step of 0.50 pH.^{49,64,65} The initial concentration of these acid, base solutions was 0.1 mol dm⁻³, the influence of the ion strength in the buffer solution on the fluorescence emission wavelength was negligible in this study.

Photostability is one of the key factors tested for responsive ability. Sensing materials irradiated under continuous

ultraviolet light usually result in a weakening fluorescence signal, but several other parameters such as emission band shape and fluorescence lifetime usually remained unchanged. The spectral and protolytic properties of the DSPs could be influenced by undergoing effective E, Z–photoisomerization under ultraviolet irradiation.⁴⁹ HPP in buffer solution of pH = 7 was irradiated under continuous ultraviolet light (250 W Hg lamp, 365 nm) for 2 h, the fluorescence intensity was decreased about 60 %; while the emission spectrum of HPP was unchanged. This implied that the fluorescent signal of HPP for pH test was not affected by UV irradiation (Figure 7S).

3 mg HPP was dispersed in 5 ml buffer solutions by the ultrasonic method and the resulting suspension solution was tested by fluorescence spectroscopy. The fluorescence spectra of the suspensions of HPP at different pH values were shown in Figure 5, the excitation wavelength of 370 nm was chosen. It is clearly observed that remarkable bathochromic shifts of the λ_{em} of HPP occurred as pH value changed from 5.5 to 1, which were assigned to the protonation process of HPP.⁴⁴ The λ_{em} of HPP at different pH values were listed in Table 1S, λ_{em} of HPP shifted from 525 to 618 nm when the pH values changed from 5.50 to 1.00. At pH = 5.50, the suspension of HPP exhibited a typical characteristic of green emitting and gradually transformed to red emitting at pH = 1.00. The photos of HPP suspension in the pH range from 1.00 to 5.50 under UV (365 nm) illumination were shown in Figure 9S. The light colors were accorded with the corresponding characteristic emissions in fluorescence spectra. However, the λ_{em} of HPP almost remained at 524 nm in the pH range from 5.50 to 12.00 (Figure 10S). The suspensions of HPP emitted a green light at the pH values from 5.50 to 12.00 under UV–irradiation (365 nm) (Figure 11S).

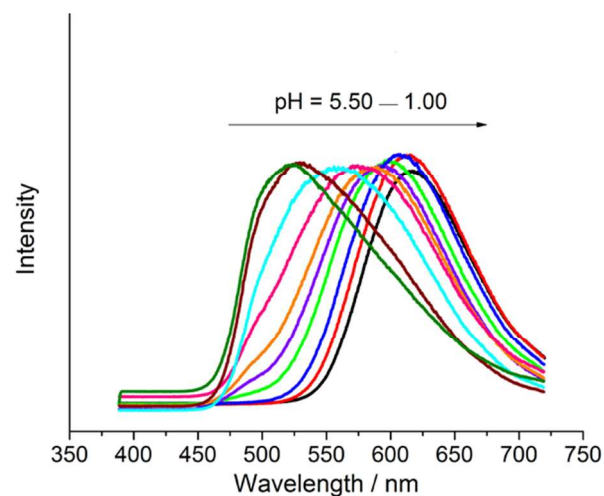
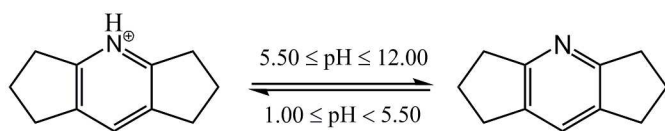


Figure 5. Fluorescence spectra of suspensions of HPP in buffer solutions with the pH in the range from 5.50 to 1.00 with interval of 0.5 pH (excited at 370 nm).

It was supposed that the pH response of HPP should be ascribed to the conversion between protonation and deprotonation states of DSP moieties.^{66,67} The pK_a value for the conjugate acid of pyridine groups were 5.25.^{66–68} This meant that the pyridyl groups were in the protonated states when pH value was below 5.25 and increasing acidity favoured the protonation of the pyridinic nitrogen atom (Scheme 2).



Scheme 2. Conformation of protonation and deprotonation for the pyridine group.

A good linear correlation between λ_{em} and pH was observed in the pH interval between 1 and 4. The correlation coefficient was 0.98 in Figure 6 and a regression formula of $pH = -0.069 \lambda_{em} + 44$ was established. This indicates that HPP could be applied as a pH indicator for acid solution, for example, gastric acid with a pH range of 1.5 to 3.5. The linear correlation coefficients were 0.96 and 0.89 as the pH values in the range of 1.00–4.50 (Figure 12S) and 1.00 – 5.00 (Figure 13S), respectively. The linear correlation coefficients were lower than 0.98 as the pH values in the range of 1.00 – 4.00, the reason that was the protonation and deprotonation of the pyridine groups coexisted at $pH = 4.50 - 5.50$. However, when pH is increased to above 5.25, deprotonation states of pyridyl groups showed no pH response and λ_{em} almost remained at 525 nm.

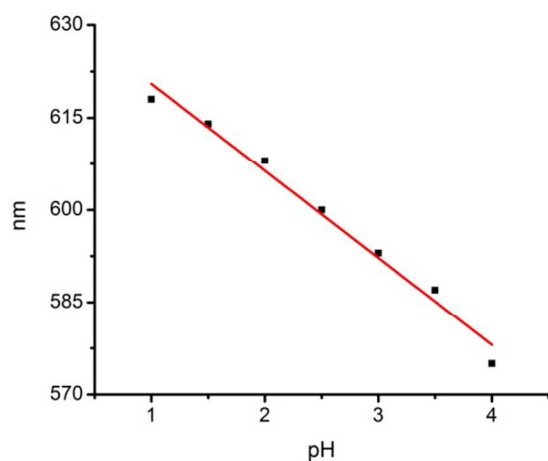


Figure 6. Plots of the fluorescence maximum emission wavelength of HPP versus pH values ($pH = 1.00 - 4.00$).

We selected two buffer solutions at $pH = 1, 12$ to investigate the recyclability of HPP. First, HPP was immersed in the buffer solution of $pH = 1$; then the above buffer solution was replaced by the buffer solution of $pH = 12$. Finally, the buffer solution of $pH = 12$ was replaced by the buffer solution of $pH = 1$ again. Each suspension of HPP was tested by fluorescence spectroscopy (Figure 14S). The fluorescence spectra of suspensions of HPP confirmed that the protonation and deprotonation of HPP was reversible, indicating that HPP could be recyclable.

Conclusions

In summary, a novel pH-responsive fluorescent nanoporous polymer has been prepared successfully through the Heck reaction by using octavinylsilsequioxane (OVS) and brominated distyrylpyridine (Br-DSP) with excellent pH-response. The porous polymer exhibited porosity with S_{BET} of $600 \text{ m}^2 \text{ g}^{-1}$ and higher CO_2 storage capability of 0.82 mmol g^{-1} (3.62 wt %) at 298 K/760 Torr. It was particularly worth mentioning that this POSS-based nanoporous polymer exhibited superior pH response, compared with other POSS-

based porous materials reported previously. PH values and the corresponding λ_{em} have a good linear relation in the pH interval between 1 and 4 ($pH = -0.069 \lambda_{em} + 44$) and the linear correlation coefficient was 0.98. This indicates that this porous polymer is very promising as a fluorescent probe in the rapid test of gastric acid, acidic waste etc..

Acknowledgements

This work was supported by the National Natural Science Foundation of China (No. 21274081).

Notes and references

^a Key Laboratory of Special Functional Aggregated Materials, Ministry of Education, School of Chemistry and Chemical Engineering, Shandong University, Jinan 250100, P. R. China. Fax: (+86)531 88364691. E-mail: liuhongzhi@sdu.edu.cn.

^b School of Chemistry and Chemical Engineering, Shanghai Jiao Tong University, 800 Dongchuan Road, Shanghai, 200240, China.

^c Key Laboratory of Specially Functional Polymeric Materials and Related Technology, Ministry of Education, East China University of Science and Technology, Shanghai, 200237.

Electronic Supplementary Information (ESI) available: Detailed experimental procedure (Br-DSP), and supplementary figures (EDS, FTIR, TGA, PXRD, FE-SEM, HR-TEM and fluorescence spectra of HPP, and ^1H NMR, solid-state ^{13}C CP/MAS NMR spectrum and mass spectrum of Br-DSP). See DOI: 10.1039/b000000x/

- 1 R. E. Morris and P. S. Wheatley, *Angew. Chem. Int. Ed.*, 2008, **47**, 4699.
- 2 Q. Chen, J. Wang, Q. Wang, N. Bian, Z. Li, C. Yan and B. Han, *Macromolecules*, 2011, **44**, 7987.
- 3 J. Schmidt, J. Weber, J. D. Epping, M. Antonietti and A. Thomas, *Adv. Mater.*, 2009, **21**, 702.
- 4 G. Soler-Illia, C. Sanchez, B. Lebeau and J. Patarin, *Chem. Rev.*, 2002, **102**, 4093.
- 5 N. B. McKeown and P. M. Budd, *Chem. Soc. Rev.*, 2006, **35**, 675.
- 6 J. X. Jiang, A. Trewin, F. Su, C. D. Wood, H. Niu, J. T. A. Jones, Y. Z. Khimiyak and A. I. Cooper, *Macromolecules*, 2009, **50**, 2658.
- 7 D. Wu, F. Xu, R. Sun, R. Fu, H. He and K. Matyjaszewski, *Chem. Rev.*, 2012, **112**, 3959.
- 8 B. Kiskan, M. Antonietti and J. Weber, *Macromolecules*, 2012, **45**, 1356.
- 9 T. Ben, K. Shi, Y. Cui, C. Pei, Y. Zuo, H. Guo, D. Zhang, J. Xu, F. Deng, Z. Tian, S. Qiu, *J. Mater. Chem.*, 2011, **21**, 18208.
- 10 A. Patra and U. Scherf, *Chem. Eur. J.*, 2012, **18**, 10074.
- 11 Y. Xu, S. Jin, H. Xu, A. Nagai and D. Jiang, *Chem. Soc. Rev.*, 2013, **42**, 8012.
- 12 A. Patra, J. Koenen and U. Scherf, *Chem. Commun.*, 2011, **47**, 9612.
- 13 K. Zhang, B. Tieke, F. Vilela and P. J. Skabara, *Macromol. Rapid Commun.*, 2011, **32**, 825.
- 14 D. Xiao, Y. Li, L. Liu, B. Wen, Z. Gu, C. Zhang and Y. S. Zhao, *Chem. Commun.*, 2012, **48**, 9519.
- 15 J. Weber and A. Thomas, *J. Am. Chem. Soc.*, 2008, **130**, 6334.
- 16 L. Chen, Y. Honscho, S. Seki and D. L. Jiang, *J. Am. Chem. Soc.*, 2010, **132**, 6742.

- 17 X. M. Liu, Y. H. Xu and D. L. Jiang, *J. Am. Chem. Soc.*, 2012, **134**, 8738.
- 18 J. X. Jiang, A. Trewin, D. J. Adams and A. I. Cooper, *Chem. Sci.*, 2011, **2**, 1777.
- 19 Y. Xu, A. Nagai and D. Jiang, *Chem. Commun.*, 2013, **49**, 1591.
- 20 Q. Chen, J. Wang, F. Yang, D. Zhou, N. Bian, X. Zhang, C. Yan and B. Han, *J. Mater. Chem.*, 2011, **21**, 13554.
- 21 R. M. Laine and M. F. Roll, *Macromolecules*, 2011, **44**, 1073.
- 22 K. Tanaka and Y. Chujo, *J. Mater. Chem.*, 2012, **22**, 1733.
- 23 C. X. Zhang, F. Babonneau, C. Bonhomme, R. M. Laine, C. L. Soles, H. A. Hristov and A. F. Yee, *J. Am. Chem. Soc.*, 1998, **120**, 8380.
- 24 J. Jiang, C. Wang, A. Laybourn, T. Hasell, R. Clowes, Y. Z. Khimiyak, J. Xiao, S. J. Higgins, D. J. Adams and A. I. Cooper, *Angew. Chem. Int. Ed.*, 2011, **50**, 1072.
- 25 W. Chaikittisilp, A. Sugawara, A. Shimojima and T. Okubo, *Chem. Mater.*, 2010, **22**, 4841.
- 26 D. Wang, L. Xue, L. Li, B. Deng, S. Feng, H. Liu and X. Zhao, *Macromol. Rapid Commun.* 2013, **34**, 861.
- 27 D. Wang, W. Yang, L. Li, X. Zhao, S. Feng and H. Liu, *J. Mater. Chem. A*, 2013, **1**, 13549.
- 28 W. Chaikittisilp, M. Kubo, T. Moteki, A. Sugawara–Narutaki, A. Shimojima and T. Okubo, *J. Am. Chem. Soc.*, 2011, **133**, 13832.
- 29 Y. Wu, D. Wang, L. Li, W. Yang, S. Feng and H. Liu, *J. Mater. Chem. A*, 2014, **2**, 2160.
- 30 W. Yang, D. Wang, L. Li and H. Liu, *Eur. J. Inorg. Chem.*, 2014, 2976.
- 31 H. Lin, J. Ou, Z. Zhang, J. Donga and H. Zou, *Chem. Commun.*, 2013, **49**, 231.
- 32 F. Alves and I. Nischang, *Chem. Eur. J.*, 2013, **19**, 17310.
- 33 N. Shanmugam, K. T. Lee, W. Y. Cheng and S. Y. Lu, *J. Polym. Sci., Part A: Polym. Chem.*, 2012, **50**, 2521.
- 34 M. F. Roll, J. W. Kampf, Y. Kim, E. Yi and R. M. Laine, *J. Am. Chem. Soc.*, 2010, **132**, 10171.
- 35 S. Zheng, H. Phillips, E. Geva and B. D. Dunietz, *J. Am. Chem. Soc.*, 2012, **134**, 6944.
- 36 H. Araki and K. Naka, *J. Polym. Sci. Part A: Polym. Chem.*, 2012, **50**, 4170.
- 37 R. M. Laine, S. Sulaiman, C. Brick, M. Roll, R. Tamaki, M. Z. Asuncion, M. Neurock, J. S. Filhol, C. Y. Lee, J. Zhang, T. Goodson, M. Ronchi, M. Pizzotti, S. C. Rand and Y. Li, *J. Am. Chem. Soc.*, 2010, **132**, 3708.
- 38 F. B. M. Suah, M. Ahmad and M. N. Taib, *Sens. Actuators, B*, 2003, **90**, 182.
- 39 T. Yazawa, S. Miyamoto, S. Yusa, T. Jin and A. Mineshige, *Mater. Res. Bull.*, 2013, **48**, 4267.
- 40 J. Wu and M. J. Sailor, *Adv. Funct. Mater.*, 2009, **19**, 733.
- 41 O. Schepelina, N. Poth and I. Zharov, *Adv. Funct. Mater.*, 2010, **20**, 1962.
- 42 H. Y. Tang, J. Guo, Y. Sun, B. S. Chang, Q. G. Ren and W. L. Yang, *Int. J. Pharm.*, 2011, **421**, 388.
- 43 R. Liu, P. H. Liao, J. K. Liu and P. Y. Feng, *Langmuir*, 2011, **27**, 3095.
- 44 H. Zhang, S. Bai, J. Sun, J. Han and Y. Guo, *Mater. Res. Bull.*, 2014, **53**, 266.
- 45 Y. F. Zhu and J. L. Shi, *Micropor. Mesopor. Mater.*, 2007, **103**, 243.
- 46 G. W. de Groot, M. G. Santonicola, K. Sugihara, T. Zambelli, E. Reimhult, J. Voros and G. J. Vancso, *ACS Appl. Mater. Interfaces.*, 2013, **5**, 1400.
- 47 X. Jiang, J. Yin, Y. Murakami and M. Kaji, *J. Photopolym. Sci. Technol.*, 2009, **22**, 351.
- 48 V. G. Pivovarenko, A. V. Grygorovych, V. F. Valuk and A. O. Doroshenko, *J. Fluoresc.*, 2003, **13**, 479.
- 49 O. V. Grygorovych, S. M. Moskalenko, B. A. Marekha and A. O. Doroshenko, *J. Fluoresc.*, 2010, **20**, 115.
- 50 V. F. Valuk, V. G. Pyvovarenko, O. V. Grygorovych and A. O. Doroshenko, *Theor. Exp. Chem.*, 2004, **40**, 256. (in Russian)
- 51 J. R. Holst, E. Stöckel, D. J. Adams and A. I. Cooper, *Macromolecules*, 2010, **43**, 8531.
- 52 E. Stöckel, X. Wu, A. Trewin, C. D. Wood, R. Clowes, N. L. Campbell, J. T. A. Jones, Y. Z. Khimiyak, D. J. Adams and A. I. Cooper, *Chem. Commun.*, 2009, 212.
- 53 D. Yuan, W. Lu, D. Zhao and H. C. Zhou, *Adv. Mater.*, 2011, **23**, 3723.
- 54 J. F. Brown, L. H. Vogt and P. I. Prescott, *J. Am. Chem. Soc.*, 1964, **86**, 1120.
- 55 D. Chen, S. Yi, W. Wu, Y. Zhong, J. Liao, C. Huang and W. Shi, *Polymer*, 2010, **51**, 3867.
- 56 I. Nischang, O. Brüggemann and I. Teasdale, *Angew. Chem. Int. Ed.*, 2011, **50**, 4592.
- 57 W. Chaikittisilp, A. Sugawara, A. Shimojima and T. Okubo, *Chem. Eur. J.*, 2010, **16**, 6006.
- 58 Y. Peng, T. Ben, J. Xu, M. Xue, X. Jing, F. Deng, S. Qiu and G. Zhu, *Dalton Trans.*, 2011, **40**, 2720.
- 59 Y. Zhao, Q. Cheng, D. Zhou, T. Wang and B. Han, *J. Mater. Chem.*, 2012, **22**, 11509.
- 60 Q. Chen, M. Luo, P. Hammershøj, D. Zhou, Y. Han, B. W. Laursen, C. Yan and B. Han, *J. Am. Chem. Soc.*, 2012, **134**, 6084.
- 61 L. Feng, Q. Chen, J. Zhu, D. Liu, Y. Zhao and B. Han, *Polym. Chem.*, 2014, **5**, 3081.
- 62 D. Wang, L. Li, W. Yang, Y. Zuo, S. Feng and H. Liu, *RSC Adv.*, 2014, **4**, 59877.
- 63 X. Jing, F. Sun, H. Ren, Y. Tian, M. Guo, L. Li and G. Zhu, *Micropor. Mesopor. Mater.*, 2013, **165**, 92.
- 64 F. Kobayashi, H. Ikeura, S. Odake, S. Tanimoto and Y. Hayata, *LWT - Food Sci. Technol.*, 2012, **48**, 330.
- 65 Y. C. Chen, R. Xie and L. Y. Chu, *J. Membr. Sci.*, 2013, **442**, 206.
- 66 J. Lindqvist, D. Nyström, E. Östmark, P. Antoni, A. Carlmark, M. Johansson, A. Hult and E. Malmström, *Biomacromolecules*, 2008, **9**, 2139.
- 67 S. Liu, L. Wang, B. Liu and Y. Song, *Polymer*, 2013, **54**, 3065.
- 68 B. Yameen, M. Ali, R. Neumann, W. Ensinger, W. Knoll and O. Azzaroni, *Nano Lett.*, 2009, **9**, 2788.